Investigations of the photochemical isotope equilibrium between O2, CO2 and O3

R. Shaheen, C. Janssen, T. Röckmann

Atmos. Chem. Phys., 7, 495–509, 2007
www.atmos-chem-phys.net/7/495/2007/

Atmospheric Chemistry and Physics

Investigations of the photochemical isotope equilibrium between O_2, CO_2 and O_3

R. Shaheen[1,2], **C. Janssen**[1,3], **and T. Röckmann**[1,4]

[1]Max-Planck-Institute for Nuclear Physics, Division of Atmospheric Physics, 69117 Heidelberg, Germany
[2]University of California San Diego, Department of Chemistry, La Jolla, USA
[3]Laboratoire de Physique Moléculaire pour l'Atmosphère et l'Astrophysique, Université Pierre et Marie Curie/CNRS, 75252 Paris, France
[4]Institute for Marine and Atmospheric Research Utrecht, Utrecht University, The Netherlands

Received: 12 June 2006 – Published in Atmos. Chem. Phys. Discuss.: 14 August 2006
Revised: 4 December 2006 – Accepted: 21 December 2006 – Published: 26 January 2007

Abstract. Contrary to tropospheric CO_2 whose oxygen isotopic composition follows a standard mass dependent relationship, i.e. $\delta^{17}O \sim 0.5\,\delta^{18}O$, stratospheric CO_2 is preferentially enriched in ^{17}O, leading to a strikingly different relation: $\delta^{17}O \sim 1.7\,\delta^{18}O$. It has been shown repeatedly that the isotope anomaly is inherited from O_3 via photolytically produced $O(^1D)$ that undergoes isotope exchange with CO_2 and the anomaly may well serve as a tracer of stratospheric chemistry if details of the exchange mechanism are understood. We have studied the photochemical isotope equilibrium in UV-irradiated O_2-CO_2 and O_3-CO_2 mixtures to quantify the transfer of the anomaly from O_3 to CO_2 at room temperature. By following the time evolution of the oxygen isotopic compositions of CO_2 and O_2 under varying initial isotopic compositions of both, O_2/O_3 and CO_2, the isotope equilibria between the two reservoirs were determined. A very strong dependence of the isotope equilibrium on the O_2/CO_2-ratio was established. Equilibrium enrichments of ^{17}O and ^{18}O in CO_2 relative to O_2 diminish with increasing CO_2 content, and this reduction in the equilibrium enrichments does not follow a standard mass dependent relation. When molecular oxygen exceeds the amount of CO_2 by a factor of about 20, ^{17}O and ^{18}O in equilibrated CO_2 are enriched by (142±4)‰ and (146±4)‰, respectively, at room temperature and at a pressure of 225 hPa, independent of the initial isotopic compositions of CO_2 and O_2 or O_3. From these findings we derive a simple and general relation between the starting isotopic compositions and amounts of O_2 and CO_2 and the observed slope in a three oxygen isotope diagram. Predictions from this relation are compared with published laboratory and atmospheric data.

Correspondence to: R. Shaheen
(robina.shaheen@mpi-hd.mpg.de)

1 Introduction

The oxygen isotopic composition of tropospheric CO_2 is determined mainly by isotope exchange with water in leaves and soils and to some extent also by exchange with ocean water and by anthropogenic emissions (Ciais et al., 1997). On average, measurements of tropospheric CO_2 show $\delta^{17}O_{VSMOW} \approx 21$‰ and $\delta^{18}O_{VSMOW} \approx 41$‰ (Thiemens et al., 1991) with seasonal and geographical variations in ^{18}O of less than 4‰ (Farquhar et al., 1993). Here, $\delta^{17}O_{VSMOW}$ and $\delta^{18}O_{VSMOW}$, respectively, denote the relative differences in the $^{17}O/^{16}O$ and in the $^{18}O/^{16}O$ ratio of a sample relative to the standard specified in the subscript, in this case Vienna Standard Mean Ocean Water (VSMOW). Note that our definition of δ values does not involve a multiplicative factor of 1000, which is in line with using ‰ as an equivalent expression for the number 10^{-3} (e.g. Mook, 2001). Tropospheric CO_2 thus follows a standard mass dependent relation with $\delta^{17}O \sim 0.5\,\delta^{18}O$. Measurements of stratospheric and lower mesospheric samples, however, revealed a significant deviation from that pattern (Thiemens et al., 1991, 1995; Lämmerzahl et al., 2002; Boering et al., 2004). δ values steadily increase with increasing altitude, resulting in peak values of $\delta^{17}O_{VSMOW}$=40.5‰ and $\delta^{18}O_{VSMOW}$=54.9 ‰ at the highest altitude (60 km) measured so far (Thiemens et al., 1995). Despite some scatter between the different measurements, all data indicate an additional enrichment of ^{17}O over ^{18}O when compared to tropospheric values. When reported relative to tropospheric CO_2 the most precise data set of stratospheric CO_2 actually suggests a very tight relationship of $\delta^{17}O_{trop-CO_2} = (1.72 \pm 0.03)\delta^{18}O_{trop-CO_2}$ (Lämmerzahl et al., 2002), indicating a very strong preferential enrichment in ^{17}O compared to ^{18}O. In order to account for the observed oxygen isotope enrichment in stratospheric CO_2 the

Published by Copernicus GmbH on behalf of the European Geosciences Union.

following reaction sequence linking CO_2 and O_3 via $O(^1D)$ was proposed (Reactions R1–R3, Yung et al., 1991) and later extended (Reaction R4, Perri et al., 2003).

$$O_3 + h\nu \rightarrow O_2 + O(^1D), \quad \lambda < 310\,\text{nm} \tag{R1}$$

$$O(^1D) + CO_2 \rightarrow CO_3^\star \tag{R2}$$

$$CO_3^\star \rightarrow O(^3P) + CO_2 \tag{R3}$$

$$CO_3^\star \rightarrow O(^1D) + CO_2 \tag{R4}$$

The rate ratio $\gamma = k_4/k_3$ between Reactions (R4) and (R3) is energy dependent (Perri et al., 2004) and favors the quenching channel ($\gamma \leq 1$) for collisional energies up to about 33 kJ/mol (Mebel et al., 2004). This scheme provides an isotope transfer from stratospheric ozone into CO_2, the former being highly and anomalously enriched in the heavy oxygen isotopes (Mauersberger et al., 2001) with the enrichment predominantly residing in the asymmetric isotopomers (Janssen, 2005). But it is presently unclear whether and where additional fractionation effects enter in these reactions or whether even another source is required to explain the oxygen isotope composition of stratospheric CO_2 (Brenninkmeijer et al., 2003).

Far reaching consequences of this stratospheric exchange mechanism on the isotopic composition of O_2 have already been demonstrated by Luz et al. (1999). In particular, the triple isotope composition of O_2 could be used as a tracer for global biospheric productivity since the anomalous loss of heavy oxygen isotopes in the stratosphere competes with the production of normal mass dependently fractionated O_2 from the biosphere on a timescale of millennia. Application to data obtained from ice cores provides a history of global biospheric productivity over the last 60 000 years (Blunier et al., 2002).

Despite the importance of the above reaction scheme, only three sets of laboratory experiments, that investigate isotope exchange between CO_2 and O_3, have been published to date. The first study used O_3-CO_2 mixtures that were irradiated with a Hg lamp (Wen and Thiemens, 1993). In this study only the O_2 isotopic composition was measured and the isotopic composition of CO_2 was inferred from the assumption of mass balance. It was confirmed that an isotope exchange via $O(^1D)$ occurs and it was further concluded that an anomalous fractionation process is associated with the excited $CO_3^\star$ intermediate, which contributes to the observed enrichments in CO_2. The second set of experiments by Johnston et al. (2000) started with mixtures of O_2 and CO_2. Hg-pen ray lamp induced photolysis of O_2 was used to produce O_3 which upon photolysis yielded $O(^1D)$ to react with CO_2. These measurements revealed the temporal evolution and the final isotopic compositions of the photochemically equilibrated CO_2 and O_2 reservoirs. Although these experiments simulate the atmospheric chemistry to the extent that O_3 is recycled through a large oxygen reservoir, the results showed a $\delta^{17}O/\delta^{18}O$ slope of 1, similar to the study of Wen and Thiemens (1993) and different from the stratospheric slope. Recently, Chakraborty and Bhattacharya (2003) have reported results that almost reproduce the stratospheric $\delta^{17}O/\delta^{18}O$ ratio of 1.7 under the experimental condition that no large oxygen reservoir as compared to ozone and carbon dioxide was present. However, it remained unclear why their particular experimental results disagree with the previous laboratory experiments, which do include the large oxygen reservoir and thus should mimic atmospheric chemistry better.

To shed additional light on the presently conflicting data base, we have investigated the isotope equilibrium properties of the UV-irradiated O_2-CO_2 system. The need for quantification of the equilibrium isotope compositions has two major reasons. Firstly, due to the UV radiation field required to produce atmospheric $O(^1D)$ in Reaction (R1), stratospheric O_3 will be in a dynamic equilibrium with O_2, where production and decomposition processes both will contribute to the isotopic composition of O_3. Experiments targeting towards understanding the stratospheric exchange chemistry therefore must aim at simulating these photochemical equilibrium conditions. Secondly, as will be shown below, the temporal evolution of CO_2 is entirely determined by the initial isotopic composition of O_2/O_3 and CO_2 and by the photochemical isotope equilibrium of the system. Knowing the latter is therefore sufficient to determine three-isotope slopes in the reaction system (R1–R4). Moreover, knowledge of the equilibrium isotope composition and its dependence on reaction parameters will allow to further restrict the isotope kinetic details of the elementary reactions involved in the above reactions. Ideally, the isotope composition of the unstable and extremely reactive $O(^1D)$ should be measured directly to understand these details. The experimental difficulties involved with this kind of measurement, however, are tremendous and it is not foreseeable when or whether accurate measurements will be possible in the future. Therefore, next to the symmetry specific measurement of ozone (e.g. Janssen and Tuzson, 2006) the equilibrium isotope composition of CO_2 is the only datum characterizing the exchange kinetics that can be measured accurately with methods presently available.

Another important motive for a systematic study is that the mixing ratio of CO_2 in O_2 is expected to have an impact on the isotope composition of CO_2. The iso-electronic (i.e., without change in the electronic configuration of the reactants) isotope exchange process (R2+R4) could possibly influence the isotopic composition of $O(^1D)$. When CO_2 is the dominant gas, this exchange should be more important than when O_2 is the dominant gas in the mixtures. Existing laboratory data were obtained under very different conditions, mostly with CO_2/O_2 much higher than in the atmosphere. Whether this implies a bias when comparing the laboratory data to the atmosphere or how large this bias could possibly be is unclear at present, which calls for a more systematic investigation.

2 Materials and methods

2.1 Setup and sample treatment

Mixtures of either CO_2 and O_2 or CO_2 and O_3 were used as starting materials for the exchange experiments. Ultra high purity CO_2 and O_2 (>99.998%, Messer Griesheim) have been used without further purification. Ozone was prepared by discharging oxygen in a commercial ozonizer (Orec V5-0, Osmonic Inc., USA). The O_2-O_3 mixture thus produced was passed through a trap at liquid N_2 temperature, allowing O_3 to condense while O_2 was pumped away. To study the isotope exchange reactions between CO_2 and O_3, CO_2 and O_2 (or O_3) were mixed in either a large spherical 2.1 L or a small cylindrical 0.25 L borosilicate reactor containing a Suprasil™ finger in the center. In the experiments reported here we used a CO_2 to O_2 ratio of roughly 1:10, since at lower CO_2 content the CO_2 isotope determination becomes increasingly more difficult and fractionation effects during extraction and measurement procedures become more important. Irradiation of the mixtures was achieved through a Hg-pen ray lamp (Oriel Instruments, Stratford, Connecticut), placed inside the Suprasil™ finger. The Hg-pen ray lamp has primary emission peaks at 184.9 and 253.7 nm and a photon flux of approximately 10^{15} photons s^{-1}. The lamp was operated at a current of 10 mA and dry nitrogen was circulated through the Suprasil™ finger to avoid UV absorption taking place outside the reactor. In some of the experiments another Hg-lamp (Puritech, Radium GmbH) with similar emission characteristics was used.

The reactor was conditioned by exposing it to ozone for several days. The same treatment was given to the connecting tubing but for a shorter time. Teflon stoppers were used in the setup in order to avoid any contamination from reaction of O_3 with Viton O-rings. At the end of each experiment CO_2 was cryogenically separated in a glass spiral trap fitted with a fiber glass thimble. The oxygen was collected on molecular sieve (13X) at 77 K. During extraction small quantities of ozone were also condensed along with CO_2. This ozone was destroyed over hot Ni foil (90±5)°C and CO_2 was separated from the product oxygen cryogenically. The effect of the decomposition of O_3 on a Ni surface was investigated in detail by Johnston et al. (2000). In their study the authors determined a slight enrichment in CO_2 from the decomposition of O_3 on Ni, which amounted to 2–3‰ for ^{17}O and ^{18}O. However, in those test experiments the amount of O_3 exceeded that of CO_2, which is due to the high $[O_2]/[CO_2]$ ratios applied there. We have used lower $[O_2]/[CO_2]$ ratios. Even for our high $[O_2]/[CO_2]\sim100$ we observed isotope material balance within (0.25±0.35)‰. Since O_3 is isotopically distinct from O_2, the good isotope material balance implies an $[O_3]/[O_2]$ ratio of $\lesssim$ 0.3%. Thus we expect that the $[O_3]/[CO_2]$ ratio was about 1 order of magnitude lower than in Johnston et al. (2000) and the effect of Ni is most likely negligible for our experiments. This conclusion is further corroborated by the results presented later in Sect. 3.2, where δO (CO_2) does not increase with $[O_2]/[CO_2]$ increasing from ∼20 to ∼120.

2.2 Preparation of enriched CO_2

Different CO_2 gases have been used to investigate the dependence of the photochemical isotope equilibrium on the isotope composition of the starting material. CO_2 enriched in either ^{17}O or ^{18}O was prepared from the combustion of synthetic mixtures of oxygen enriched in the respective heavy oxygen isotopes on activated charcoal. The enriched oxygen gas was prepared by mixing pure $^{17}O_2$ (>90 atom-%, Isotec Inc.) and $^{18}O_2$ (>99 atom-%, Isotec Inc.) with normal tank oxygen. Random distribution of heavy isotopes in the oxygen mixture was achieved by discharging the mixture for one hour in a stainless steel cylinder. The system to produce CO_2 from O_2 consisted of a pyrex glass reactor. Activated charcoal pellets were filled in a platinum mesh cup, which itself was placed inside a cup made out of sheathed thermocouple used as a heater element. The temperature was controlled with an additional thermocouple sensor. The combustion system was described in detail by Röckmann (1998). Before combustion the carbon reactor was heated to ∼800°C while being evacuated. When oxygen was admitted to the evacuated system at ∼650°C, it quickly reacted with carbon to form CO_2 that was trapped at liquid nitrogen temperature at the bottom of the reactor. The conversion of O_2 to CO_2 was monitored by a pressure gauge. Conversion was complete when the pressure in the reactor was less then 1 hPa and did not change any more. This final pressure was higher than the pressure observed prior to the introduction of oxygen, because CO, which does not condense at 77 K, forms during combustion in trace amounts. After conversion of O_2 to CO_2, the heating was switched off and the reactor was cooled to ∼200°C to prevent the interaction of resultant CO_2 with the hot reactor walls and to avoid the formation of CO during the transfer of CO_2 to a sample bottle. The CO_2 produced was then dried over P_2O_5 and further purified in multiple freeze thaw cycles, i.e. by pumping away non condensable components from CO_2 at liquid N_2 temperature.

Altogether, three different CO_2 gases have been used. Tank CO_2, ^{17}O enriched CO_2 and ^{18}O enriched CO_2, which were named CO_2-I, CO_2-II and CO_2-III, respectively. The oxygen isotopic composition was $\delta^{17}O$=13.0‰, $\delta^{18}O$=25.1‰ (CO_2-I), $\delta^{17}O$=102.1‰, $\delta^{18}O$=51.6‰ (CO_2-II) and $\delta^{17}O$=21.0‰, $\delta^{18}O$=172.3‰ (CO_2-III) for the experiments starting from O_2 and CO_2, with all values given with respect to VSMOW. For the O_3-CO_2 experiments a slightly different mixture of CO_2-II ($\delta^{17}O$=103.6 ‰, $\delta^{18}O$=36.3‰) was used. The accuracy of the δ values for the starting CO_2 material is 0.6 and 0.2‰ for ^{17}O and ^{18}O, respectively.

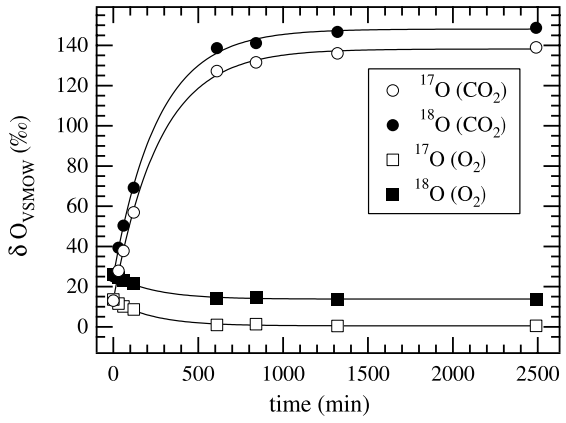

Fig. 1. Oxygen isotope changes in O_2 (squares) and CO_2 (circles) as a function of time at a constant ratio of $[O_2]/[CO_2]$ ∼12±1. Open and solid symbols refer to ^{17}O and ^{18}O, respectively. The lines indicate exponential fits according to Eq. (1) to the data. CO_2-I and O_2 with $\delta^{17}O_{VSMOW}$=13.6‰ and $\delta^{18}O_{VSMOW}$=26.2‰ were used.

2.3 Mass spectrometric analysis

A dual inlet isotope ratio mass spectrometer (Thermo Finnigan, Delta Plus^{XL}) with multiple cup detectors was used to determine the isotopic composition of CO_2 and O_2. The ^{17}O content of CO_2 was measured using the CeO_2 exchange method (Assonov and Brenninkmeijer, 2001). The method involves measurement of the CO_2 isotopic composition twice, i.e. before and after equilibration of the carbon dioxide with the oxygen adsorbed on CeO_2 at ∼650°C for 35 min. The accuracy of the method was verified using CO_2 of various isotopic compositions: CO_2 I–III and CO_2 enriched in both ^{17}O and ^{18}O. Reproducible results were obtained with all different types of CO_2. A typical scatter in $\delta^{17}O$ of 0.6 ‰ (2σ) was observed during all exchange experiments, which is taken as the analytical error.

2.4 Blank experiments

To test the possibility of fractionation induced from processes other than photochemically induced isotope exchange (e.g. fractionation during sample extraction, impurities or wall effects), two types of blank experiments were performed. (i) Pure CO_2 (∼100 µmol) was kept in the reactor for 30 min and extracted back afterwards. The results indicated negligible fractionation from sample handling. (ii) Mixtures of CO_2 and O_2 were kept in the reactor for long times (approximately 64 h) without operating the lamp. Data indicated a negligible fractionation for oxygen ($\delta^{17}O$=−0.06‰, $\delta^{18}O$=0.03‰). Also for CO_2 the observed isotope change of ($\delta^{17}O$=0.4‰, $\delta^{18}O$=0.2‰) is of the same magnitude as the measurement accuracy (Sect. 2.3) and thus errors introduced through the sample treatment and recovery are not significant.

3 Results

The typical time evolution of the isotopic compositions of CO_2 and O_2 in an isotope exchange experiment is shown in Fig. 1, where a mixture of (64±1) µmol CO_2 and (800±10) µmol O_2 in the small reactor was irradiated with a Hg lamp for various time intervals. With increasing reaction time CO_2 gets enriched in the heavy isotopes, while O_2 gets depleted. Following an exponential time dependence, the isotope compositions approach their plateau values:

$$\delta(t) = \delta_{eq} - \left(\delta_{eq} - \delta_i\right) \exp\left(-t/\tau\right) . \quad (1)$$

Here δ_i and δ_{eq} are the initial and equilibrium δ values. t is the irradiation time and τ the e-folding time of the equilibration process, i.e., the time after which the difference $(\delta_{eq} - \delta_i)$ is reduced to 1/e of its initial value.

No measurable change in CO_2 isotopic composition is observed when the mixture is exposed to irradiation times longer than about 2–5 days, somewhat depending on the lamp performance. Isotope enrichment in CO_2 is accompanied by a corresponding depletion in O_2. Owing to mass conservation, the depletion in the large O_2 reservoir is about 12 times smaller than the enrichment in CO_2. If plotted on a conventional three-isotope plot, the data of Fig. 1 define arrays with a slope of 1.01±0.02 for the heavy isotope enrichment in CO_2.

3.1 Photochemical isotope equilibrium

In order to further establish the concept of photochemical isotope equilibrium and to investigate its dependence on the initial isotopic composition of CO_2, the three CO_2 gases (I–III) with greatly differing isotopic compositions have been utilized. Experiments with O_2-CO_2 mixtures were conducted with CO_2 in the range from 0.04 to 0.06 mmol and O_2 varying from 0.5 to 1 mmol. The corresponding molar ratios ρ=$[O_2]/[CO_2]$ were kept at values between 12 and 17 and the mixtures were irradiated for up to ∼6 days. The results of these measurements are summarized in Table 1.

To investigate the isotope equilibrium between CO_2 and O_2 it is useful to report the isotopic composition of CO_2 directly with reference to the O_2 at the same time during the experiment, rather than versus the international standard VSMOW. For reasons of completeness we also report values with reference to VSMOW in Table 1. However, we mostly use $\delta^{17}O_{O_2}(CO_2)$ and $\delta^{18}O_{O_2}(CO_2)$ from here on and we note that this is an uncommon usage of the δ notation, since it implies that the "reference ratio" in the definition of the δ value is not a fixed ratio but changes itself. Nevertheless, those units help us to elucidate the exchange process since they show the evolution of the isotopic composition of the reactants relative to each other, not relative

Table 1. Oxygen isotope composition using different initial CO_2 gases (I–III) and molecular oxygen or ozone. δ values are given on the common VSMOW scale. CO_2 values are also given with O_2 as the reference gas.

O_2/O_3	CO_2 Type	$\delta O_{VSMOW}(O_2)$ (‰)		$\delta O_{VSMOW}(CO_2)$ (‰)		$\delta O_{O_2}(CO_2)$ (‰)	
		^{17}O	^{18}O	^{17}O	^{18}O	^{17}O	^{18}O
O_2	CO_2-I	13.6	26.2	13.0	25.1	−0.6	−1.0
		11.6	24.3	27.8	39.4	16.0	14.7
		10.1	23.0	37.8	50.3	27.3	26.8
		8.6	21.5	56.9	69.2	47.9	46.7
		0.9	14.2	127.2	138.7	126.1	122.7
		1.3	14.8	131.6	141.2	130.1	124.6
		0.4	13.7	136.0	146.7	135.5	131.2
		0.5	13.7	139.0	148.7	138.5	133.2
	CO_2-II	3.8	7.4	102.1	51.6	98.0	44.0
		−0.5	1.4	138.9	134.8	139.4	133.2
	CO_2-III	3.8	7.3	21.1	174.3	17.2	165.7
		−5.9	8.4	117.5	147.8	124.1	138.2
		−7.4	7.4	130.6	141.8	139.0	133.4
O_3	CO_2-I	71.3	94.7	13.0	25.1	−54.5	−63.5
		71.1	94.0	25.4	39.0	−42.7	−50.2
		69.4	92.1	26.9	40.1	−39.8	−47.6
		75.7	98.8	27.9	40.8	−44.4	−52.8
		75.4	98.2	29.4	43.7	−42.8	−49.6
		68.9	91.7	54.4	68.7	−13.6	−21.1
		59.6	82.5	155.0	172.4	90.1	83.1
		60.7	83.4	179.2	198.1	111.7	105.9
	CO_2-II	77.7	101.8	103.1	35.7	23.6	−59.9
		57.3	73.5	190.3	203.5	125.8	121.1
		59.8	77.2	200.7	210.0	132.9	123.3
	CO_2-III	79.8	101.6	21.0	173.8	−54.4	65.5
		78.1	99.7	38.2	172.7	−37.0	66.4
		60.6	88.5	185.6	221.4	117.9	122.1
		62.9	90.5	193.8	227.5	123.2	125.7

to an international scale. These enrichments of CO_2 with respect to O_2 are shown in Fig. 2a, where the data are displayed in a three-isotope plot. The exponential time evolution of an individual mixture, such as the one shown in Fig. 1, traces out a linear array on the three-isotope plot. Regardless of the initial CO_2 isotopic composition, CO_2 approaches a common isotopic composition with ongoing irradiation. At this point, the entire chemical system (O_2, electronically excited oxygen $O_2(^1\Delta)$, O_3, $O(^3P)$, $O(^1D)$ and CO_2) is in a kinetically driven, dynamic isotope equilibrium. A simultaneous least square fit on all data reveals that CO_2 in photochemical isotope equilibrium is almost equally enriched in both heavy isotopes. With respect to O_2 the values are $\delta^{17}O_{O_2}(CO_2)$=(139±1)‰ and $\delta^{18}O_{O_2}(CO_2)$=(134±1)‰.

In the second set of experiments, where mixtures of ozone and carbon dioxide were utilized, the amount of CO_2 ranged from 0.06 to 0.07 mmol and O_3 (expressed in terms of O_2 equivalents) varied in the range between 0.7 and 1.1 mmol, with corresponding molar ratios ρ in the range from 8 to 12. The CO_2-O_3 mixtures were irradiated with the Oriel Hg-pen ray lamp between 20 min and 5 days. The enrichments in CO_2 after reaction with O_3 are shown in a three-isotope plot (Fig. 2b). Again, linear arrays that evolve towards a common point are observed. For these specific experimental conditions, equilibrated CO_2 is enriched by $\delta^{17}O_{O_2}(CO_2)$=(134±6) ‰ and $\delta^{18}O_{O_2}(CO_2)$=(128±4)‰ with respect to the final oxygen, again irrespective of the initial CO_2 isotopic composition. These equilibrium values are also derived from the intersection of the fit lines.

3.2 Dependence on $[O_2]/[CO_2]$

Several series of experiments were conducted at a fixed pressure (225±10 hPa) and different O_2/CO_2 ratios (ρ) varying in the range from 0.2 to 117 to investigate the dependence of the equilibrium enrichments on ρ. The experiments were conducted in a small reactor at ambient temperature using a Puritech lamp for photolysis. In these experiments, the time evolution of the oxygen isotopic composition of CO_2 and O_2

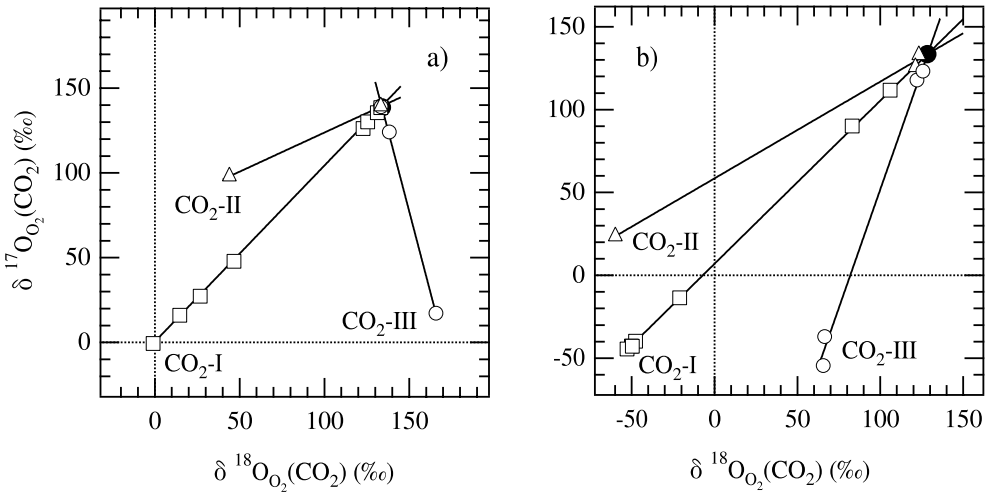

Fig. 2. (a) Three-isotope evolution arrays for the three different CO_2-O_2 mixtures. Open squares, triangles and circles represent experiments with different initial CO_2 (I–III). The solid circle marks the common point of isotope equilibration, that is inferred from a simultaneous least square fit to the data (represented by the three solid lines). The slopes of the fit lines are included in Table 2. Dotted lines define δO=0. **(b)** Evolution arrays for the CO_2-O_3 mixtures. The same symbols as in (a) are used. All axes are to the same scale and δ values are given with reference to the instantaneous isotope composition of molcular oxygen in the mixture.

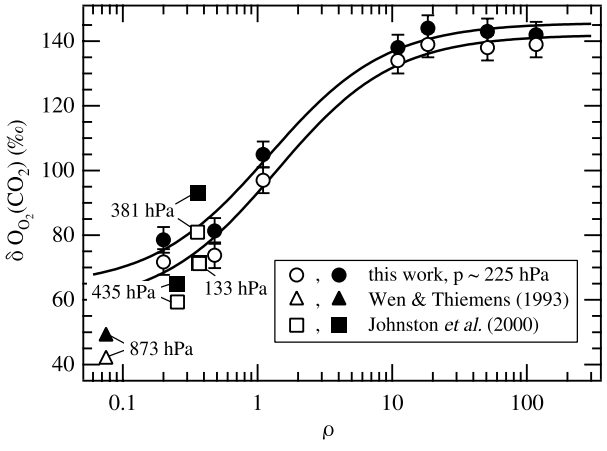

Fig. 3. Dependence on the mixing ratio ρ=[O_2]/[CO_2]. ^{17}O and ^{18}O containing CO_2 is represented by open and solid symbols, respectively. Data are at constant pressure $p\sim$225 hPa (see Table 2) and error bars denote 2 σ uncertainties. Comparison with data from the literature is indicated and the particular pressure conditions of these measurements are noted. Solid lines describe the weighted average of two a-priori unknown isotopic sources with relative weights $1/(1+\rho/\rho_0)$ and $(\rho/\rho_0)/(1+\rho/\rho_0)$, according to Eq. (2).

under varying O_2/CO_2 ratios was followed and exponential fits according to Eq. (1) were applied to the data series. The results obtained are summarized in Table 2 and displayed in Fig. 3.

The figure shows that the magnitude of enrichment in CO_2 does indeed depend strongly on ρ. A marked transition between the CO_2 ($\rho<1$) and the O_2 ($\rho>1$) dominated region is observed. In the high O_2 regime, plateaus of the CO_2 enrichments are clearly established, with $\delta^{17}O_{O_2}(CO_2)$ and $\delta^{18}O_{O_2}(CO_2)\sim 140\ldots145$‰. From this plateau of high enrichments at $\rho\geq 20$, the enrichment decreases by roughly 40‰ for ^{17}O and ^{18}O until $\rho=1$ and continues to decrease to a possible second plateau below $\rho=0.1$. For the highest relative content of CO_2 that we have measured ($\rho=0.20$), δ^{17}O and δ^{18}O are already diminished by about 60‰ with respect to the high O_2 plateaus, respectively. Introducing the symbol X for the equilibrium δ values $\delta^{17}O_{O_2}(CO_2)$ and $\delta^{18}O_{O_2}(CO_2)$, we can describe the dependency on ρ as

$$X(\rho) = \frac{1}{1+\rho/\rho_0} X_l + \frac{\rho/\rho_0}{1+\rho/\rho_0} X_h. \quad (2)$$

X_l and X_h denote the CO_2 equilibrium compositions in the low and high O_2 regimes, respectively, with the low O_2 plateaus being less accurately determined by our measurements. ρ_0 characterizes the transition between the two regimes and denotes the ratio where the enrichment takes the average value of X_l and X_h. A fit to the data returns the following numbers (errors given on a 95% confidence level): X_l=(58±11)‰, X_h=(142±4)‰ and ρ_0=1.38±0.71 for ^{17}O and X_l=(64±11)‰, X_h=(146±4)‰ and ρ_0=1.23±0.65 for ^{18}O. Within error limits, the transition between the two regimes occurs for equal amounts of O_2 and CO_2.

Table 2. Effect of $[O_2]/[CO_2]$ ($=\rho$) on the CO_2 equilibrium isotopic composition. Equilibrium $\delta_{O_2}(CO_2)$ values are denoted by X. X and the e-folding time constant τ for equilibration have been derived from fits using Eq. (1). Errors are given on the 95 % confidence level. Note that the time constants are about 2 to 3 times larger than the one of the experiment displayed in Fig. 1. This is due to the use of a different photolysis lamp.

Experiment	Pressure	ρ	^{17}O		^{18}O	
No	(hPa)		X (‰)	τ (min)	X (‰)	τ (min)
143-SR	224±10	1.1	97±3	1430±120	105±3	1430±130
144-SR	230±10	18	139±4	1630±150	144±4	1680±140
145-SR	228±12	51	138±4	1000±170	143±4	1090±130
146-SR	228±12	117	139±4	1110±200	142±4	1120±200
147-SR[a]	230±10	11	134±4	–	138±4	–
148-SR[a]	220±10	0.20	72±4	–	79±4	–
149-SR[a]	220±10	0.48	74±4	–	81±4	–

a: equilibrium values derived from an individual long time run

4 Discussion

The results from our isotope triangulation experiments clearly indicate that when a mixture of O_2/O_3 and CO_2 is irradiated with UV light, the system will evolve towards an isotope equilibrium, in which O_2 and CO_2 have a fixed isotopic relation. The exchange mechanism can at least qualitatively be explained by Reactions (R1–R4). At isotope equilibrium, the CO_2 before and after isotope exchange with $O(^1D)$ does no longer differ in isotopic composition.

In the three-isotope plots of Fig. 2, strikingly different slope values are observed between the O_2 and the O_3 experiments for mixtures starting with almost the same initial CO_2. This is due to initial O_3 and O_2 having completely different isotopic compositions in the two sets of experiments. In the set I experiments, the initial O_2 is mass dependently fractionated ($\delta^{17}O_{VSMOW}$=(3.7±0.3)‰ and $\delta^{18}O_{VSMOW}$=(7.3±0.1)‰), and O_3 formation starts from a normal oxygen reservoir. This is similar to atmospheric conditions. In the set II experiments we have anomalously fractionated oxygen available for secondary O_3 formation ($\delta^{17}O_{VSMOW}(O_3)$=(78±3)‰ and $\delta^{18}O_{VSMOW}(O_3)$=(101±3)‰). Note that in our experiments almost all of the initial O_3 in set II is converted to O_2 after ∼3 min of photolysis ($J(O_3)\sim10^{-2}\,s^{-1}$). This leads to different positions of the various CO_2 gases relative to O_2 in the three-isotope plots. For example, the slope for CO_2 enriched in ^{18}O (CO_2-III) is −3.8 in Fig. 2a and +2.9 in Fig. 2b, because in the O_2-CO_2 experiments the initial $\delta^{18}O$ of CO_2-III is higher than at photochemical equilibrium, whereas in the O_3-CO_2 experiment the initial $\delta^{18}O$ of (CO_2-III) is lower than at photochemical isotope equilibrium. Nevertheless, the photochemical equilibrium between CO_2 and O_2 appears to be almost the same in the two sets of experiments. The equilibrated CO_2 in the O_3-CO_2 experiment is ∼5‰ less enriched compared to the O_2-CO_2 experiment. Such slight differences in the observed equilibrium enrichment values are likely due to the slight differences in total pressure and in the O_2/CO_2 mixing ratio, as discussed below. We conclude that the CO_2 isotopic composition at photochemical equilibrium is independent of the initial O_2 and CO_2 isotopic composition.

Note that this only holds for isotope mixtures of low heavy isotope abundance (which includes near-natural isotope abundances and the normal or anomalous enrichments of the order of few hundred ‰ as used in our experiments). The limit to the statement is that the isotope chemistry should be determined by singly substituted species only, e.g. $^{18}O(^1D)$ should only be produced by singly substituted O_3. In strongly enriched mixtures, a departure from this behavior is expected. For example, in 50:50 mixtures of ^{16}O and ^{18}O, heteronuclear heavy isotopomers, $^{16}O_2{}^{18}O$ and $^{16}O^{18}O_2$, are similarly enriched by about 10% with respect to O_2. Homonuclear $^{16}O_3$ and $^{18}O_3$, however, do not show such an isotope effect (Mauersberger et al., 1993; Janssen et al., 2003). For illustrative purposes we assume that they are not fractionated at all. As a first approximation we now consider only isotope effects due to the abundance of O_3 molecules. Then, $^{16}O_3$ and $^{18}O_3$ produce $^{16}O(^1D)$ and $^{18}O(^1D)$ at equal amounts, as $^{16}O_2{}^{18}O$ and $^{16}O^{18}O_2$ do also. Therefore, the expected $^{18}O(^1D)/^{16}O(^1D)$ ratio is exactly 1 and $^{18}O(^1D)$ will not be enriched. This is strikingly different from natural oxygen mixtures, where $^{18}O(^1D)$ comes from $^{16}O_2{}^{18}O$ only. Since that is strongly enriched, $^{18}O(^1D)$ will be too. In addition – though likely smaller in magnitude – there are even more factors that could cause a dependence on the initial isotopic composition when changing the isotope composition of the reactants from slightly to heavily enriched: isotope dependent quenching efficiencies of $O(^1D)$ and $CO_3^\star$ ozone isotopomer dependent photolysis rates and mass dependent rates of the $O(^1D)$ + CO_2 reaction, which would include reactions with $C^{18}O_2$, for example.

4.1 Dependence on $[O_2]/[CO_2]$

Our experiments with varying the O_2/CO_2 ratio at constant pressure show that the ^{17}O and ^{18}O equilibrium enrichments in CO_2 decrease when the CO_2 content exceeds 5%. This may imply that the presence of CO_2 itself has an effect on the final equilibrium. On the one hand, it is possible that the higher stabilization efficiency of CO_2 compared to O_2 or N_2 in the formation of O_3 ($\sim$2.7 Guenther et al., 2000) leads to a 2.7 times larger effective pressure (610 at ρ=0 instead of 225 hPa). Analysing available (Morton et al., 1990; Thiemens and Jackson, 1990) and new data on the effect of pressure on the isotope effects in ozone formation, this would correspond to a reduction of the equilibrium values by 17‰ and 22‰ for ^{17}O and ^{18}O, respectively (Tuzson and Janssen, 2007, see also Eq. 11). No direct experimental data on ozone isotope enrichments in a CO_2 bath are available and data on isotopomer specific rate coefficients in ozone formation (Guenther et al., 2000) do neither support nor disprove this hypothesis. While such an effect would qualitatively agree with the observations, it is not sufficient to quantitatively explain the strong dependency on ρ.

Another mechanism through which CO_2 could directly affect the isotope equilibrium is the non-quenching exchange channel between CO_2 and $O(^1D)$. If sufficient $O(^1D)$ is exchanged with CO_2 via this channel (i.e. at high CO_2 abundance), CO_2 itself provides an isotopic source of $O(^1D)$ and can alter the isotopic composition of the $O(^1D)$ reactant. Thus, our findings may provide evidence for isotope exchange between CO_2 and $O(^1D)$ on a singlet surface as observed during recent cross molecular beam experiments (Perri et al., 2003). Note, however, that CO_2 is never a direct source of $O(^1D)$. Therefore, even in CO_2 dominated mixtures where CO_2 is the primary reaction partner of $O(^1D)$, the branching ratio between Reactions (R4) and (R3) determines the maximum fraction of $O(^1D)$ that originates from CO_2. Because of its energy dependence (Perri et al., 2004; Mebel et al., 2004) and because of the unknown energy distribution of $O(^1D)$ under our experimental conditions, the branching ratio between Reactions (R4) and (R3) is uncertain. O_3 photolysis at 254 nm provides hot $O(^1D)$ with roughly 54 kJ/mol kinetic energy, which in N_2 or O_2 is only partly thermalized before electronic quenching occurs (Takahashi et al., 2002). From the Monte-Carlo simulations of Takahashi et al. (2002), we estimate a typical $O(^1D)$-CO_2 collisional energy of 8 kJ/mol in O_2 dominated mixtures. Even though thermalisation in reactive CO_2 collisions is very efficient because a large fraction ($\sim$60%) of the available energy is deposited in CO_2 (Perri et al., 2003), $O(^1D)$ is likely to be hotter in CO_2 dominated mixtures, because of the $\sim 11/4$ higher quenching efficiency of CO_2 compared to O_2 (Sander et al., 2003). Hence, the effective collisional energy could be as much as 20 kJ/mol, leading to relatively high values of $\gamma \sim 25\%$ as compared to a lower value of only 5% in the oxygen bath (Mebel et al., 2004). With changing branching ratios going from high to low O_2 content, isotope effects in Reactions (R3) and (R4) could very well lead to an additional variation between high and low O_2 regimes.

A very interesting result of the ρ-dependence study is that the equilibrium enrichments for ^{17}O and ^{18}O decrease towards lower values of ρ in a 1:1 fashion. This decrease cannot be attributed to isotope changes in O_3, thus we observe an anomalous fractionation signal that must have another origin. Therefore, this observation is experimental evidence for an anomalous fractionation step in the processes that are responsible for the decrease from the high-ρ plateau.

4.2 Isotope equilibrium and three-isotope correlations

Our experiments clearly show that it is not sufficient to exclusively discuss slopes in three-isotope plots for characterization of the O_3-CO_2 exchange. Obviously, the slopes depend strongly on the isotopic composition of the starting gases, as already indicated for CO_2 by Chakraborty and Bhattacharya (2003). This must be kept in mind when comparing slope data from different experimental series. The experiments with artificially enriched gases (CO_2 and O_2) presented here demonstrate that in fact the photochemical equilibrium point is an inherent property of the exchange process which provides the underlying information to obtain three-isotope slopes. Here we show how three-isotope slopes depend on the equilibrium point and the initial CO_2 and O_2 isotopic compositions.

We use the isotope equilibrium point from the CO_2-O_2 exchange experiments and denote the equilibrium composition of CO_2 by $^{17}X = \delta^{17}O_{O_2}(CO_2)$, $^{18}X = \delta^{18}O_{O_2}(CO_2)$. To keep the notation short and simple, superscripts to denote isotopes ^{17}O or ^{18}O are omitted wherever possible. We thus write δ instead of $\delta^{17}O$ or $\delta^{18}O$, and likewise, X to denote both, ^{17}X and ^{18}X. Indices i and f denote initial and final, equilibrated compositions, respectively. We start with the standard scale conversion equation that expresses $\delta_{O_2}(CO_2)$ in terms of $\delta_{VSMOW}(O_2)$ and $\delta_{VSMOW}(CO_2)$.

$$\delta_{O_2}(CO_2) = \frac{\delta_{VSMOW}(CO_2) - \delta_{VSMOW}(O_2)}{1 + \delta_{VSMOW}(O_2)} . \quad (3)$$

With the above definition of X, this can be rearranged to relate final O_2 to CO_2 and X, with δ values of both compounds defined on the VSMOW scale:

$$\delta_{VSMOW}(O_{2,f}) = \frac{\delta_{VSMOW}(CO_{2,f}) - X}{1 + X} \quad (4)$$

For the remainder of this Sect. 4.2 we can drop the subscript on the δ values, because we are concerned with a single standard, VSMOW in our case. Nevertheless, the derivation holds for any standard substance, such as for air oxygen, for example.

Using square brackets to denote molecular number densities and assuming that ozone levels are small enough to be neglected, conservation of mass requires that

$\Delta\delta(CO_2)\,[CO_2]+\Delta\delta(O_2)\,[O_2]=0$, where $\Delta\delta$ denotes the change in the δ value during an experiment. Equivalently, when relative amounts $\rho=[O_2]/[CO_2]$ are introduced, mass conservation implies the following relation between initial (i) and final (f) delta values:

$$\delta(CO_{2,i}) + \rho\ \delta(O_{2,i})=\delta(CO_{2,f}) + \rho\ \delta(O_{2,f}). \quad (5)$$

It is interesting to note that this leads to identical three-isotope slopes for both, the O_2 and the CO_2 evolution arrays, because for changes Δ in $\delta^{17}O$ and $\delta^{18}O$ we find

$$\frac{\Delta\delta^{17}O(CO_2)}{\Delta\delta^{18}O(CO_2)} = \frac{\Delta\delta^{17}O(O_2)}{\Delta\delta^{18}O(O_2)}. \quad (6)$$

Upon combining Eqs. (4) and (5), the isotopic composition of equilibrated CO_2 on the VSMOW scale can entirely be determined in terms of the initial composition of the mixture (ρ, $\delta(CO_{2,i})$, $\delta(O_{2,i})$) and X:

$$\delta(CO_{2,f})=X + \frac{(1+X)\left\{\delta(CO_{2,i}) + \rho\ \delta(O_{2,i})-X\right\}}{1+X+\rho} \quad (7)$$

For the slope of $\delta(CO_2)$ in the three-isotope plot, $m=\left\{^{17}\delta(CO_{2,f})-{}^{17}\delta(CO_{2,i})\right\} / \left\{^{18}\delta(CO_{2,f})-{}^{18}\delta(CO_{2,i})\right\}$ we finally obtain

$$m = \frac{^{18}\delta(O_{2,i})-{}^{18}\delta(CO_{2,i}) + {}^{18}X\left\{1+{}^{18}\delta(O_{2,i})\right\}}{^{17}\delta(O_{2,i})-{}^{17}\delta(CO_{2,i}) + {}^{17}X\left\{1+{}^{17}\delta(O_{2,i})\right\}} \times\frac{1+\rho+{}^{18}X}{1+\rho+{}^{17}X}\,. \quad (8)$$

This expresses m in terms of the reactants and the equilibrium fractionation values between CO_2 and O_2, ^{17}X and ^{18}X, provided the ozone concentration is small enough to be neglected in the total mass balance. We note that m in Eq. (8) becomes dependent on ρ through the mass balance relation (5) and through the dependence of X on ρ. The direct dependence on ρ in the second factor of Eq. (8), however, will be weak under experimental conditions, because ^{17}X and ^{18}X are not only significantly smaller than 1, but also similar in value, such that this factor remains close to 1 for all values of ρ.

4.3 Dependency on $[O_2]/[CO_2]$-ratio and pressure

It is expected that both, ^{17}X and ^{18}X, also show a pressure and temperature dependency. At least, isotope fractionation in ozone formation does so and $O(^1D)$, being a photo-product of O_3, is likely to reflect this. These dependencies should therefore be investigated for a complete description of the isotope equilibrium. For comparison with previous laboratory results, however, only the pressure dependency needs to be known, because temperature conditions in the experiments were always at room temperature or slightly higher, perhaps. Some temperature rise above ambient is likely due to heating by the photolysis light sources used in all the experiments.

In the absence of pressure dependent data, we assume that the pressure dependence of X is solely caused by changing the pressure conditions of ozone formation. New pressure dependent measurements and already published data (Morton et al., 1990; Thiemens and Jackson, 1990) on ozone isotope enrichments at room temperature have been combined and simultaneously analyzed (Tuzson and Janssen, 2007). They obey the following empirical pressure dependence between 7 and 20 000 hPa:

$$\delta O_{O_2}(O_3)(p) = A + B\Big/\sqrt{1+p/p_0}\,, \quad (9)$$

where A is a pressure independent offset, B is the change in the fractionation going from high to low pressures and p_0 is pressure at which the transition occurs. Allowing for different offset values A for the different data sets that might be due to slight temperature differences and different fractionation effects in photolytic ozone decomposition, the following set of parameters reproduce the data within ±9‰ (1σ=3.6‰): B=113.3‰ and p_0=1230 hPa for ^{17}O and B=137.8‰ and p_0=1150 hPa for ^{18}O. This pressure dependency describes the isotopic composition of ozone formed in the gas phase. At low pressures, ozone formation at wall surfaces contributes (Bains-Sahota and Thiemens, 1987; Morton et al., 1990; Tuzson and Janssen, 2006) and leads to negative deviations from Eq. (9). Those deviations are normal mass dependent and become significant at pressures around 10 hPa in a 2.5 l reaction volume (Morton et al., 1990) and at higher pressures in smaller reactors.

Because of strong experimental evidence that all pressure induced variability in ozone enrichments is due to the asymmetric ozone species alone (Tuzson and Janssen, 2007), $O(^1D)$ enrichments will show pressure variations that are 3/2 times the effects in ozone itself. Given that $\delta O_{O_2}(O(^1D))(p)=Y(p)$ is known for some pressure p_a, we can predict the pressure dependence of the equilibrium composition on the basis of the ozone isotope effect alone

$$Y(p) = Y(p_a) + \frac{3B}{2\sqrt{1+p/p_0}}\left(1-\sqrt{\frac{1+p/p_0}{1+p_a/p_0}}\right). \quad (10)$$

The second term on the left hand side describes the pressure dependency of the $O(^1D)$ isotopic composition, which will determine the equilibrium isotope composition of CO_2. The same pressure dependency is thus expected for the CO_2 equilibrium composition

$$X(p) = X(p_a) + \frac{3B}{2\sqrt{1+p/p_0}}\left(1-\sqrt{\frac{1+p/p_0}{1+p_a/p_0}}\right), \quad (11)$$

but the above mentioned limitations due to ozone wall formation must be kept in mind.

4.4 Comparison with laboratory data

Equation (8) relates three-isotope slopes directly to the photochemical equilibrium point, provided that the isotopic

composition of the initial reactants is known. We can now apply this equation and the hypothesized pressure dependence of X (Eq. 11) to our triangulation experiments that were carried out at lower pressures as well as to previous measurements reported in the literature. Since the isotope equilibrium point is a general property of the isotope exchange system, any laboratory or atmospheric exchange process should evolve towards this equilibrium point. If other conditions (i.e. temperature, photolysis wavelengths) are similar, we expect that our formalism can reproduce the experimental results. Conversely, if experimental results deviate from our prediction, this is a clear indication of either experimental problems or fundamentally different experimental conditions.

4.4.1 Low pressure experiments

First, we compare our low pressure triangulation experiments ($\sim$9 hPa) to the ρ dependence study at 225 hPa. Table 3 shows that even when the difference in pressure is accounted for according to Eq. (11), the predicted enrichments are $\sim$25‰ higher for ^{18}O and $\sim$10‰ for ^{17}O than the measured ones. Those differences are robust, since they are similar for the CO_2-O_2 and CO_2-O_3 experiments, which were performed at almost the same pressure. This is a clear indication that additional factors contribute in the low pressure experiments. Interestingly, the differences behave in an almost standard mass dependent way. As discussed in Sect. 4.3, a mass dependent depletion relative to the calculation points towards the influence of wall effects in ozone formation. Thus, we attribute the differences to wall effects, which are indeed expected to become important at these low pressures, even in the 2 l spherical reactors employed (see discussion above).

Since the absolute equilibrium enrichments are large compared to the mismatch between computation and measurement, the predictions for the slope still reflect the general trend of the observations. The values of the CO_2 three-isotope slopes strongly vary with the initial isotope composition of O_2 and CO_2, between -3.8 and $+2.9$ in our experiments. The predicted slopes get highly uncertain when the values of the numerator or denominator of the first term in Eq. (8) are close to 0. An error of just 0.0005 (corresponding to measurement uncertainties of less than 0.5‰) in the initial or final isotope compositions leads to the error estimates given in Table 3. On the other hand, small errors for the calculated CO_2 slopes indicate little sensitivity to measurement uncertainties (i.e. initial or final isotope compositions).

4.4.2 Johnston et al. (2000) experiments

Turning to previously published data, we find that the 435 hPa data point of Johnston et al. (2000) agrees very well with our prediction. The 381 hPa data point does not fit into this scheme because it is more enriched than our data. However, the mass balance relation (Eq. 5) between CO_2 and O_2 is violated in this experiment (see Table 1 in Johnston et al., 2000). When we correct the O_2 data to satisfy isotope mass balance, the corrected values bring this particular point almost in agreement with our prediction, including the three-isotope slope. Mass balance is also violated for the 133 hPa data point (see Table 1 in Johnston et al., 2000), but here the discrepancy cannot be solved by attributing the mass balance error to O_2. The discrepancy is also reflected in different three-isotope slopes for the O_2 and CO_2 evolution arrays. While CO_2 has a slope >1, the slope for O_2 is 0.94. Yet, mass balance between O_2 and CO_2 (Eq. 5) implies identical slopes. We note that for the 435 hPa data point, the observed three-isotope slopes of O_2 and CO_2 agree prefectly with each other and with the calculated slope. The ten oxygen data indicate a slope of 0.89 with a scatter less than 0.01, whereas the individual CO_2 data show a larger scatter around the same average value.

Johnston et al. (2000) also performed $\delta^{18}O(CO_2)$ measurements at very high ρ (between 720 and 950) for 100, 400 and 800 hPa. The value of $\delta^{18}O_{O_2}(CO_2)$=113‰ at 100 hPa is already significantly lower than our high oxygen plateau at 225 hPa. One has to keep in mind, however, that measurements at low CO_2 content become challenging due to small sample sizes. Johnston et al. (2000) reported substantial amounts (up to 20%) of "excess" CO_2 in the samples. The origin of this excess CO_2 remains unexplained. Thus, a quantitative correction is impossible, but any contamination from ambient CO_2 would lead to diminished $\delta^{18}O(CO_2)$ values. The higher pressure δ values of Johnston et al. (2000) qualitatively show the predicted behavior, i.e. decreasing enrichments with increasing pressures. Nevertheless, since all those high ρ data appear to suffer from contamination we cannot use them for quantitative comparison.

4.4.3 Wen and Thiemens (1993) experiments

Only one data point of Wen and Thiemens (1993, Table 1) is included in Fig. 3, because the remaining measurements in their Table 1 (covering a range of ρ from 0.065 to 8.5) appear to not have reached isotope equilibrium. The data all lie below our measurements and get closer with increasing irradiation times. The equilibrium data point of Wen and Thiemens (1993) can be reproduced within 14‰. Given the large uncertainty of our prediction for small values of ρ (11‰ at the 95% level of confidence), this is almost satisfactory as is the agreement between measured and calculated slopes. Nevertheless, we cannot exclude that the slight discrepancy may have an experimental origin. Wen and Thiemens (1993) placed the light source outside the reactor, whereas we determined the equilibrium point used for the calculation with a light source in the reactor. This likely causes temperature differences between the experimental setups. Ozone isotopomer enrichments increase with temperature (Morton et al., 1990; Janssen et al., 2003) and a 10‰ difference in

Table 3. Comparison of CO_2 equilibrium predictions with previously observed data obtained from experiments employing Hg lamp O_3 photolysis. If not noted otherwise, δ values are given with reference to VSMOW and the slope of the CO_2 signatures is calculated using values on the VSMOW scale. Most experiments in the literature don't provide information on the equilibrium, but on the slope of the CO_2 evolution array. Error estimates for observed and calculated slopes are given in parentheses. When available, observed error estimates are given as 2σ values resulting from linear fits to the data and uncertainties for calculated values derive from an uncertainty of 0.0005 in both, the numerator and denominator of the first term given in Eq. (8).

Ref.	p (hPa)	ρ	initial CO_2 (‰)		initial O_2/O_3 (‰)		$\delta^{17}O_{O_2}(CO_2)$ (‰)		$\delta^{18}O_{O_2}(CO_2)$ (‰)		CO_2 slope	
			$\delta^{17}O$	$\delta^{18}O$	$\delta^{17}O$	$\delta^{18}O$	obs.	calc.	obs.	calc.	obs.	calc.
a	8.6	15	13.0	25.1	3.7	7.3	139	148	134	157	1.03(1)	1.00(8)
a	8.6	15	102.0	51.6	3.7	7.3	139	148	134	157	0.45(2)	0.44(8)
a	8.6	15	21.2	174.0	3.7	7.3	139	148	134	157	−3.8(1)	−14.(13)
b	10	10	13.0	25.1	77	99	134	145	128	154	0.99(4)	0.91(3)
b	10	10	104.0	36.3	77	102	134	145	128	154	0.58(1)	0.55(3)
b	10	10	21.1	174.0	80	103	134	145	128	154	2.9(2)	2.2(1)
c, d	133	0.369	5.7	11.0	8.3	16.0	71.2	81	71.5	90	1.05(7)	0.88(1)
c, e	381	0.358	5.7	11.0	8.3	16.0	73.5	73	72.8	68	0.92(7)	0.90(1)
c	435	0.254	5.7	11.0	8.3	16.0	59.3	61	65.1	65	0.89(4)	0.90(1)
f	873	0.065	1.3	5.3	23.1	44.7	41.6	36	48.7	35	0.72	0.75(1)
f, g	457	0.13	1.3	5.3	23.1	44.7	–	54	–	58	0.73	0.76(1)
f, g	175	0.44	1.3	5.3	23.1	44.7	–	81	–	89	0.77	0.78(1)
f, g	113	0.89	1.3	5.3	23.1	44.7	–	97	–	107	0.84	0.80(1)
f, g	69	3.3	1.3	5.3	23.1	44.7	–	127	–	136	0.92	0.83(2)
f, g	57	8.5	1.3	5.3	23.1	44.7	–	140	–	148	0.95	0.84(3)
h	3	8.0	20.4	39.3	105.9	124.9	–	143	–	153	1.8	0.95(2)
h	3	8.0	2.2	4.1	105.9	124.9	–	143	–	153	1.5	0.90(2)
h	3	8.0	−5.6	−10.9	105.9	124.9	–	143	–	153	1.3	0.88(2)

a: this work, set I experiments starting with CO_2-O_2.
b: this work, set II experiments starting with CO_2-O_3.
c: Johnston et al. (2000), experiments started with CO_2-O_2.
d: Mass balance for ^{18}O is violated in this particular data set.
e: Final O_2 values corrected assuming mass balance. Uncorrected values yield $\delta^{17}O_{O_2}(CO_2)$ =80.9‰ and $\delta^{18}O_{O_2}(CO_2)$=93.0‰.
f: Wen and Thiemens (1993), experiments started with CO_2-O_3, slope determined from δ (O_2), initial $\delta O(CO_2)$ is suspect, because $\delta^{17}O \neq 0.52\,\delta^{18}O$. We assume $\delta^{17}O(CO_2)$=2.8‰, corresponding to a working standard of 19.7 instead of 17.9‰.
g: equilibrium was not reached, but changes in $\delta(O_2)$ exceeded 10‰.
h: Chakraborty and Bhattacharya (2003), start with CO_2-O_3, equilibrium not reached.

^{18}O requires a temperature difference of only 20 K. This is not unrealistic given the different experimental configurations and the variations we have observed when different lamps were employed. Exploring the role of temperature in determining the isotope equilibrium is one of the most pressing tasks for future investigation.

For the experiments of Wen and Thiemens (1993) that did not reach isotope equilibrium, we can nevertheless compare the three-isotope slopes. Table 3 contains the data that showed robust changes in the isotope composition of O_2 by more than 10‰ for both ^{17}O and ^{18}O. The measurements show a much stronger trend in three-isotope slopes than our calculations. This mismatch is most likely due to the above mentioned uncertainties in the low pressure extrapolation. Because of the very small reactor dimensions (76 cm^3), wall effects should be very pronounced here. Note, that an additional standard mass dependent depletion in ozone would lead to an increase in slope values, as observed.

On the experimental side, it should be noted that the observed slope values become more uncertain with decreasing pressures due to the experimental method employed. With increasing oxygen content of the mixture, changes in the isotopic composition of O_2 become smaller and the relative errors of the measurements that determine the accuracy of the three-isotope slope increase. For the 57 hPa measurement of Wen and Thiemens (1993) an error of only 1‰ in ^{17}O would lead to an error of 0.1 in the CO_2 three-isotope slope and thus would suffice to explain the discrepancy between observed and calculated values.

4.4.4 Chakraborty and Bhattacharya (2003) experiments

The data discussed so far are at least reasonably consistent with our photochemical equilibrium calculations. This does not hold for the data of Chakraborty and Bhattacharya (2003), which cannot at all be explained by our calculations

(see Table 3). Such a strong discrepancy indicates fundamental differences in the experimental conditions, and several factors may contribute.

First, the O_3 used for these experiments was produced differently (photolysis and condensation at liquid N_2 temperature). Isotope fractionation during O_3 formation is strongly temperature dependent (Morton et al., 1990; Janssen et al., 2003). However, this alone cannot explain the large difference, since the O_3 isotopic composition reported in Chakraborty and Bhattacharya (2003) was not very much different from ours. Moreover, the effect of having different initial isotope compositions should have no effect when the system is driven into equilibrium, because initial isotopic compositions are fully taken into account by using δ values relative to O_2.

Secondly, Chakraborty and Bhattacharya (2003) did not use a large reservoir of O_2 but started their experiments with O_3. This is similar to the set-II experiments discussed above, but also in those experiments we got results consistent with our other findings. However, in our experimental setup the initial O_3 was converted to O_2 within three minutes. Slower O_3 conversion was reported in the experiments of Chakraborty and Bhattacharya (2003). If O_3 is present at high concentrations during the short-duration experiments, it is the dominant buffer gas, because it reacts faster with $O(^1D)$ than CO_2 (2.4 vs. 1.1×10^{-10} cm^3 s^{-1}, Sander et al., 2003). This could affect the isotopic composition and kinetic energy distribution of $O(^1D)$and via the energy dependent branching ratio between Reactions (R3) and (R4) on the isotopic composition of $O(^1D)$ and thus CO_2. High ozone concentrations can also affect the isotope photochemistry through absorption. If only 50% of the initial ozone was decomposed, radiation at 253.7 nm would be effectively shielded. Under the experimental conditions of Chakraborty and Bhattacharya (2003) the penetration depth is just 2 cm, about ten times smaller than the diameter of the reactor. Using typical intensities for Hg-discharge lamps (Reader et al., 1996; Mentges, 2006) and the wavelength dependence of the photolysis cross section in the Hartley band of ozone (Sander et al., 2003; Miller et al., 2005) we estimate that photolysis at 184.9 nm becomes dominant after about 6 . . . 13 cm of penetration, the lower value at the beginning of the experiment, the higher when half of the initial ozone has been decomposed. To some extent ($\sim$10%) photolysis at 312.5/313.1 nm may also contribute. In particular around 310 nm, extraordinarily large isotope effects in ozone photodissociation have been predicted (200‰ for $^{18}O_3$ Miller et al., 2005), which is much larger than the typically inferred value of $<$20‰ for photodecomposition of ^{18}O containing ozone at 253.7 nm (Brenninkmeijer et al., 2003). Presently, the role of UV photodecomposition on the isotopic composition of ozone has not been investigated thoroughly in experiments. However, a strong wavelength dependence as suggested by Miller et al. (2005) could explain why the equilibrium and non-equilibrium experiments show strikingly different results.

Thirdly, in the kinetic experiments by Chakraborty and Bhattacharya (2003), the O_3 isotopic composition is almost entirely determined by the formation process. $O(^1D)$ derived therefrom will acquire the isotopic composition of (asymmetric) ozone *plus* the effect in the photodecomposition process. In equilibrium experiments (Wen and Thiemens, 1993; Johnston et al., 2000, this work), however, O_3 will acquire its isotopic composition from both processes, formation and photolytic decomposition. In this case $O(^1D)$ essentially carries the isotopic composition of (asymmetric) ozone in the formation process *without* any contribution from an isotope effect in the photodissociation of ozone, because the latter effect cancels identically. If, contrary to earlier evidence (Brenninkmeijer et al., 2003), isotope effects in the photochemical decomposition of O_3 are large (Miller et al., 2005), also large differences between kinetic and equilibrium effects are expected. More experimental data on ozone photodecomposition and detailed kinetic modeling is required to establish this assertion.

We close our discussion of previous laboratory data with the remark that experiments in the past either appear to suffer from experimental deficiencies at high O_2/CO_2 ratios or have been performed at small values of ρ. Our experiments show that in this case the results are effected by the high levels of CO_2 not present in the atmosphere. Moreover, in low pressure experiments, including our own triangulation measurements, heterogeneous ozone formation at surface appears to contribute, so that the results cannot be directly transferred to the atmospheric situation.

4.5 Atmospheric implications

We can apply Eq. (8) in combination with Eq. (11) to stratospheric conditions, using the isotopic compositions of tropospheric CO_2 and O_2 as the initial values. We infer a $\delta^{17}O/\delta^{18}O$ slope of 1.0 for stratospheric CO_2 – independent of pressure in the range between 5 and 100 hPa. Thus, application of the photochemical equilibrium equation to the atmosphere does not reproduce the stratospheric $\delta^{17}O/\delta^{18}O$ slope of 1.7 (see Fig. 4). This indicates that in order to understand the atmospheric data as well as to get complete insight into the exchange mechanism, other parameters such as wavelength dependent photolysis of ozone as well as temperature need to be addressed. The temperature dependence of the isotope effect in ozone formation (Morton et al., 1990) could possibly account for some of the differences. With decreasing temperatures and decreasing δ values, the ratio $\delta^{17}O/\delta^{18}O$ in ozone increases. Assuming everything else remaining unchanged, this will lead to an isotopic composition of $O(^1D)$ that is situated above the line between the origin and room temperature $O(^1D)$ in a three-isotope diagram. Thus, the slope for the CO_2 array should indeed increase with decreasing temperature.

In the absence of experimental evidence on the effects of temperature on the exchange process, we suggest an

additional or alternative explanation for the discrepancy. The isotopic composition of O_3 in the atmosphere is affected by both, formation and photodecomposition. Measurements, however, show that the isotopic composition in the lower and middle stratosphere can be explained by the isotope effect in the formation process only (Mauersberger et al., 2001; Liang et al., 2006). This leaves little room for large fractionation effects in ozone decomposition in the lower stratosphere and indeed, laboratory experiments indicate that broadband ozone photolysis in the visible region (Chappuis band) should cause only small isotope effects (e.g. Brenninkmeijer et al., 2003). Recent remote sensing measurements (Haverd et al., 2005) suggest that large photolytic isotope effects may be effective at higher altitudes ($\gtrsim$35 km) where UV photolysis of ozone is important. If this is true, $O(^1D)$, which is produced via UV photolysis, may effectively deviate from the isotopic composition of (asymmetric) ozone, which itself is not affected much at lower altitudes due to the much more efficient photolysis in the Chappuis band. As discussed above, such a situation may in fact be mimicked by the experiments of Chakraborty and Bhattacharya (2003), where ozone was produced under conditions where UV decomposition can be neglected and where ozone photolysis to produce $O(^1D)$ was likely not quantitative to change the isotope composition of ozone significantly. However, this is certainly different to our experimental conditions where ozone photodissociation and production of $O(^1D)$ occur at the same wavelength and where UV photolytic isotope fractionation will have an influence on the isotope composition of ozone. Note that this explanation requires small isotope effects in the photodecomposition of ozone at wavelengths that do not produce $O(^1D)$ and a comparatively large fractionation in the photolysis step that produces isotopically light $O(^1D)$ while heavy isotopes would be enriched in ozone. Qualitatively this requirement is in agreement with the calculations of Miller et al. (2005).

In order to explain their observations, Chakraborty and Bhattacharya (2003) also discussed additional isotope effects, which would lead to an CO_2 equilibrium point that deviates from asymmetric ozone. They proposed that the $O(^1D) + CO_2$ reaction could introduce a large isotope effect (~ -50‰ for ^{18}O) by considering hard sphere collisional frequencies for that reaction. While our experiments actually indicate that large isotope effects are indeed associated with the $O(^1D) + CO_2$ reaction, these effects are most likely too complex to be accounted for in a simple hard sphere collisional model, not alone given the energy dependent branching ratio between iso-electronic exchange and quenching. Model calculations have already demonstrated (Johnston et al., 2000) that consistent use of collisional frequency factors will lead to very small net effects in CO_2 ($\sim$1‰ for ^{18}O), because a similar isotope effect occurs in the competing reactions that lead to the removal of $O(^1D)$. Thus $^{16}O(^1D)$ is removed preferentially, increasing the steady state concentration of $^{18}O(^1D)$ available for reaction with CO_2. This way collisional frequency effects cancel almost completely. The same argument applies to the atmosphere, where $O(^1D)$ is controlled by quenching with N_2 and O_2.

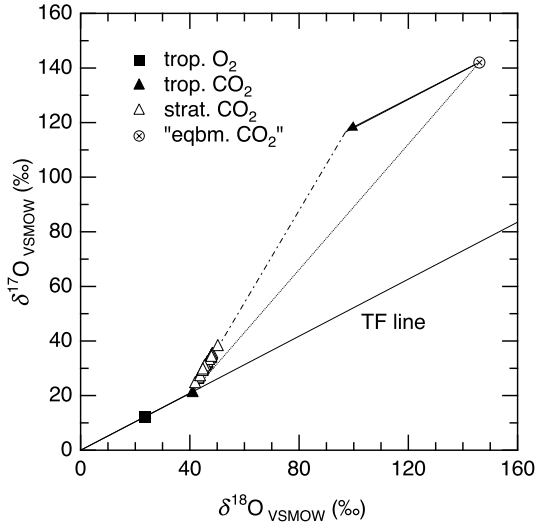

Fig. 4. Comparison between predicted (dotted line) and observed (open triangles/slash-dotted line) stratospheric CO_2 arrays. Trop. CO_2 (Thiemens et al., 1991), strat. CO_2 (Lämmerzahl et al., 2002). Based on the discrepancy an additional isotope effect (arrow) is assumed that leads to a shifted equilibrium position.

Comparing our laboratory based results to the atmospheric three-isotope slope of CO_2, we can estimate the magnitude of the hypothesized fractionation process, provided that it follows a standard mass dependency. Our formalism predicts an equilibrium isotopic composition of stratospheric CO_2 of $\delta^{17}O_{VSMOW}$=142‰ and $\delta^{18}O_{VSMOW}$=146‰ at 50 hPa. In order to recover the atmospheric slope of 1.7, the equilibrated stratospheric CO_2 must be shifted roughly by -50‰ along a slope 0.52 line in the three isotope plot. This is the magnitude of the fractionation process that is missing in our experiments and it agrees with the number inferred by Chakraborty and Bhattacharya (2003). The fractionation can tentatively be attributed to preferential UV photodecomposition of heavy ozone, but we note that other effects have been neglected. Firstly, part of the observed discrepancy between asymmetric ozone and equilibrium CO_2 can likely be attributed to the temperature dependence of the isotope effects in ozone formation. Secondly, a possible fractionation from photolysis in the Chappuis band may have to be included. Finally, the presence of N_2 in the atmosphere could make some difference, because it is less efficient in quenching $O(^1D)$ than O_2.

5 Conclusions

We have shown that the isotope composition of CO_2 at photochemical isotope equilibrium with oxygen and ozone is

independent of the initial isotopic composition of CO_2 and O_2 used. Most importantly, the photochemical isotope equilibrium is an inherent property of the isotope exchange system. By studying this equilibrium point, we gain more relevant insight about the exchange process than by just studying three-isotope slopes which are obviously dependent on the initial isotopic compositions of the reactants. In fact, we show that if the isotope equilibrium point is known, three-isotope slopes can be readily calculated from the initial isotopic composition of the reactants. Thus experiments that help to characterize precisely the dependencies of the isotope equilibrium point on reaction parameters will likely advance our understanding of three-isotope slopes observed in the laboratory and in the atmosphere.

We have investigated the role of the O_2/CO_2 ratio for the $O(^1D)$ mediated isotope transfer between O_3 and CO_2. We indeed found a strong dependence of the isotope equilibrium on the O_2/CO_2 ratio. This implies that CO_2 itself may affect the exchange process, for example via non-quenching exchange with $O(^1D)$. However, this exchange will not be relevant for the atmosphere with very high O_2/CO_2 ratios. Although a deeper understanding of the exchange mechanism has now been obtained, our results do not offer an explanation for the stratospheric three-isotope slope of 1.7. This clearly indicates that other parameters like temperature and ozone photolysis wavelength, some of which are well known to produce large effects in the isotopic composition of ozone, need to be addressed in future studies in order to understand the isotopic composition of stratospheric CO_2. In particular, we suggest that multi-wavelength ozone photo-dissociation effects could possibly explain the discrepancy with the atmospheric observations. The proposed mechanism also appears to be in accordance with the only study that has reported such a slope close to 1.7 (Chakraborty and Bhattacharya, 2003). However, as long as this hypothesis has not been veryfied, we must conclude that the origin of the striking isotopic composition of stratospheric carbon dioxide remains an open question.

Acknowledgements. This work is part of the project ISOSTRAT, funded by the German ministry of education and research (BMBF) within the AFO 2000 program (grant number 07ATC01). We would like to thank B. Knape for his assistance to maintain high standards of measurements on the mass spectrometer. The unfailing support of P. Franz and M. Brass to solve all sorts of software problems is highly acknowledged. We appreciate the help of S. Assonov for providing some CO_2 samples and B. Tuzson for preparing enriched mixtures of oxygen. Thanks are due to J. Janicke, R. Albert, U. Schwan, F. Kepler for useful discussions and providing a friendly working environment. R. Shaheen would particularly like to acknowledge the assistance of P. But, chairman PAEC, Islamabad, Pakistan, who enabled her to complete this work. Last but not least we are thankful to both referees, C. Brenninkmeijer and M. Miller, for their insightful comments and stimulating remarks.

Edited by: M. Ammann

References

Assonov, S. S. and Brenninkmeijer, C. A. M.: A new method to determine the ^{17}O isotopic abundance in CO_2 using oxygen isotope exchange with a solid oxide, Rapid Communications in Mass Spectrometry, 15, 2426–2437, 2001.

Bains-Sahota, S. K. and Thiemens, M. H.: A Chemically Produced Non-Mass Dependent Sulfur Isotope Effect, Meteoritics, 22, 320–321, 1987.

Blunier, T., Barnett, B., Bender, M. L., and Hendricks, M. B.: Biological oxygen productivity during the last 60,000 years from triple oxygen isotope measurements, Global Biogeochem. Cycles, 16, 1029, doi:10.1029/2001GB001460, 2002.

Boering, K. A., Jackson, T., Hoag, K. J., Cole, A. S., Perri, M. J., Thiemens, M., and Atlas, E.: Observations of the anomalous oxygen isotopic composition of carbon dioxide in the lower stratosphere and the flux of the anomaly to the troposphere, Geophys. Res. Lett., 31, L03109, doi:10.1029/2003GL018451, 2004.

Brenninkmeijer, C. A. M., Janssen, C., Kaiser, J., Röckmann, T., Rhee, T. S., and Assonov, S. S.: Isotope effects in the chemistry of atmospheric trace compounds, Chem. Rev., 103, 5125–5161, 2003.

Chakraborty, S. and Bhattacharya, S. K.: Experimental investigation of oxygen isotope exchange between CO_2 and $O(^1D)$ and its relevance to the stratosphere, J. Geophys. Res., 108, 4724, doi:10.1029/2002JD002915, 2003.

Ciais, P., Denning, A. S., Tans, P. P., Berry, J. A., Randall, D. A., Collatz, G. J., Sellers, P. J., White, J. W. C., Trolier, M., Meijer, H. A. J., Francey, R. J., Monfray, P., and Heimann, M.: A three-dimensional synthesis study of $\delta^{18}O$ in atmospheric CO_2. 1. Surface fluxes, J. Geophys. Res., 102, 5857–5872, 1997.

Farquhar, G. D., Lloyd, J., Taylor, J. A., Flanagan, L. B., Syvertsen, J. P., Hubick, K. T., Wong, S. C., and Ehleringer, J. R.: Vegetation effects on the isotope composition of oxygen in atmospheric CO_2, Nature, 363, 439–443, 1993.

Guenther, J., Krankowsky, D., and Mauersberger, K.: Third-body dependence of rate coefficients for ozone formation in ^{16}O-^{18}O mixtures, Chem. Phys. Lett., 324, 31–36, 2000.

Haverd, V., Toon, G. C., and Griffith, D. W. T.: Evidence for altitude-dependent photolysis-induced ^{18}O isotopic fractionation in stratospheric ozone, Geophys. Res. Lett., 32, L22808, doi:10.1029/2005GL024049, 2005.

Janssen, C.: Intramolecular isotope distribution in heavy ozone ($^{16}O^{18}O^{16}O$ and $^{16}O^{16}O^{18}O$), J. Geophys. Res., 110, D08308, doi:10.1029/2004JD005479, 2005.

Janssen, C. and Tuzson, B.: A diode laser spectrometer for symmetry selective detection of ozone isotopomers, Appl. Phys. B, 82, 487–494, 2006.

Janssen, C., Guenther, J., Krankowsky, D., and Mauersberger, K.: Temperature dependence of ozone rate coefficients and isotopologue fractionation in ^{16}O-^{18}O oxygen mixtures, Chem. Phys. Lett., 367, 34–38, 2003.

Johnston, J. C., Röckmann, T., and Brenninkmeijer, C. A. M.: CO_2+$O(^1D)$ isotopic exchange: Laboratory and modeling studies, J. Geophys. Res., 105, 15 213–15 229, 2000.

Lämmerzahl, P., Röckmann, T., Brenninkmeijer, C. A. M., Krankowsky, D., and Mauersberger, K.: Oxygen isotope composition of stratospheric carbon dioxide, Geophys. Res. Lett., 12, 1582, doi:10.1029/2001GL014343, 2002.

Liang, M. C., Irion, F. W., Weibel, J. D., Miller, C. E., Blake, G. A.,

and Yung, Y. L.: Isotopic composition of stratospheric ozone, J. Geophys. Res., 111, D02 302, doi:10.1029/2005JD006342, 2006.

Luz, B., Barkan, E., Bender, M. L., Thiemens, M. H., and Boering, K. A.: Triple-isotope composition of atmospheric oxygen as a tracer of biosphere productivity, Nature, 400, 547–550, 1999.

Mauersberger, K., Morton, J., Schueler, B., Stehr, J., and Anderson, S. M.: Multi-Isotope Study of Ozone - Implications for the Heavy Ozone Anomaly, Geophys. Res. Lett., 20, 1031–1034, 1993.

Mauersberger, K., Lämmerzahl, P., and Krankowsky, D.: Stratospheric ozone isotope enrichments – revisited, Geophys. Res. Lett., 28, 3155–3158, 2001.

Mebel, A. M., Hayashi, M., Kislov, V. V., and Lin, S. H.: Theoretical Study of Oxygen Isotope Exchange and Quenching in the $O(^1D) + CO_2$ Reaction, J. Phys. Chem. A, 108, 7983–7994, http://dx.doi.org/10.1021/jp049315h, 2004.

Mentges, J.: Line sources, technical data sheet, http://www.lot-oriel.com/site/site_down/ls_calibration_deen03.pdf, 2006.

Miller, C. E., Onorato, R. M., Liang, M. C., and Yung, Y. L.: Extraordinary isotopic fractionation in ozone photolysis, Geophys. Res. Lett., 32, L14814, doi:10.1029/2005GL023160, 2005.

Mook, W. G., ed.: Environmental Isotopes in the Hydrological Cycle: Principles and Applications, vol. I, IAEA, http://www.iaea.org/programmes/ripc/ih/volumes/volumes.htm, 2001.

Morton, J., Barnes, J., Schueler, B., and Mauersberger, K.: Laboratory studies of heavy ozone, J. Geophys. Res., 95, 901–907, 1990.

Perri, M. J., Van Wyngarden, A. L., Boering, K. A., Lin, J. J., and Lee, Y. T.: Dynamics of the $O(^1D) + CO_2$ oxygen isotope exchange reaction, J. Chem. Phys., 119, 8213–8216, 2003.

Perri, M. J., Van Wyngarden, A. L., Lin, J. J., Lee, Y. T., and Boering, K. A.: Energy dependence of oxygen isotope exchange and quenching in the $O(^1D) + CO_2$ reaction: A crossed molecular beam study, J. Phys. Chem. A, 108, 7995–8001, 2004.

Reader, J., Sansonetti, C. J., and Bridges, J. M.: Irradiances of spectral lines in mercury pencil lamps, Appl. Opt., 35, 78–83, 1996.

Röckmann, T.: Measurement and interpretation of ^{13}C, ^{14}C, ^{17}O and ^{18}O variations in atmospheric carbon monoxide, Ph.D. thesis, University of Heidelberg, 1998.

Sander, S. P., Friedl, R. R., Golden, D. M., Kurylo, M. J., Huie, R. E., Orkin, V. L., Moortgat, G. K., Ravishankara, A. R., Kolb, C. E., Molina, M. J., and Finlayson-Pitts, B. J.: Chemical Kinetics and Photochemical Data for Use in Atmospheric Studies, Evaluation Number 14, JPL Publication 02-25, 2003.

Takahashi, K., Taniguchi, N., Sato, Y., and Matsumi, Y.: Nonthermal steady state translational energy distributions of $O(^1D)$ atoms in the stratosphere, J. Geophys. Res., 107, ACH 6-1–ACH 6-6, 2002.

Thiemens, M. H. and Jackson, T.: Pressure Dependency for Heavy Isotope Enhancement in Ozone Formation, Geophys. Res. Lett., 17, 717–719, 1990.

Thiemens, M. H., Jackson, T., Mauersberger, K., Schueler, B., and Morton, J.: Oxygen isotope fractionation in stratospheric CO_2, Geophys. Res. Lett., 18, 669–672, 1991.

Thiemens, M. H., Jackson, T., Zipf, E. C., Erdman, P. W., and Van Egmond, C.: Carbon Dioxide and Oxygen Isotope Anomalies in the Mesosphere and Stratosphere, Science, 270, 969–972, 1995.

Tuzson, B. and Janssen, C.: Unambiguous identification of ^{17}O containing ozone isotopomers for symmetry selective detection, Isotopes Environ. Health Studies, 42, 67–75, 2006.

Tuzson, B. and Janssen, C.: Temperature and Pressure Dependence of Ozone Isotopomer Formation: A Symmetry Resolved Study, in press, 2007.

Wen, J. and Thiemens, M. H.: Multi-Isotope Study of the $O(^1D)+CO_2$ Exchange and Stratospheric Consequences, J. Geophys. Res., 98, 12 801–12 808, 1993.

Yung, Y. L., DeMore, W. B., and Pinto, J. P.: Isotopic Exchange between Carbon Dioxide and Ozone Via $O(^1D)$ in the Stratosphere, Geophys. Res. Lett., 18, 13–16, 1991.